Teaching Thermal Design of Power Electronic Systems with Web-Based Interactive Educational Software

Uwe DROFENIK and Johann W. KOLAR

Power Electronic Systems Laboratory
Swiss Federal Institute of Technology (ETH) Zurich
ETH-Zentrum / ETL, CH-8092 Zurich, Switzerland
Phone: +41-1-632-4267, Fax: +41-1-632-1212
E-mail: drofenik@lem.ee.ethz.ch, kolar@lem.ee.ethz.ch

Abstract. For designing reliable power electronic systems it is essential to understand basic thermal issues like the stationary and transient relation of the power semiconductor losses the junction temperature and the application of thermal equivalent circuits. Also, thermal properties are of special importance in connection with further increasing the compactness of power converter systems. The aim of this paper is to give an introduction into the basic theory of heat energy conduction and thermal design which should serve as an addition to the Java applets compiled in a the *iPES-Thermal*, a module of the interactive educational software *iPES* which is freely available at www.ipes.ethz.ch and employed at the ETH Zurich for supporting an introductory course on power electronics.

1 Introduction

1.1 Thermal Problems in Power Electronics

In lectures on fundamentals of power electronics thermal design is often neglected because the focus is traditionally on circuits, topologies and control. Therefore, students often do not have a clear understanding of the importance of a proper thermal design of power electronic systems.

This paper should compile lecture material providing an introduction into the basics of thermal issues relevant to power electronics. The paper is complimentary to Java applets of the interactive educational software *iPES* (*Interactive Power Electronics Seminar*) which also will be discussed in this paper.

1.2 Interactive Power Electronics Seminar (*iPES*)

The *Interactive Power Electronics Seminar (iPES)* [1], [2] available at www.ipes.ethz.ch at no costs is an effort to make educational software interactive by employing Java applets. Different power electronic circuits are shown with animated current-flow in dependency of operating parameters like load-resistance or input-voltage. The user can click with the mouse directly into the circuit elements and signal for changing parameters, and the corresponding changes of the time-behavior or other diagrams are shown immediately. The focus of *iPES* is not on simulation but on interactive animation. Currently available educational modules are "*iPES-Cicuits*", "*iPES-Advanced Circuits*" and "*iPES-Electromag-netics*" and "*iPES-Thermal"* which will be in the focus in the following.

2 Heat Conduction

2.1 Heat Conduction in Power Electronic Systems

In general there are three basic heat transfer mechanisms: heat conduction, convection and radiation [3].

In a medium the heat transfer is by lattice oscillations and electrons (for conductive materials). This mechanism, denominated as heat conduction is of paramount importance in power electronic applications, and will be discussed in detail in this paper.

Power losses occurring inside a power semiconductor are finally conducted to a heat sink surface, i.e. a convective interface. In natural convection the heat is conducted to the surrounding medium via a thin boundary layer. There, the heat energy does change the adjacent medium density where the created buoyancy causes the medium to flow. For significantly increasing this mechanism of heat transfer the mass flow could be created by fans, i.e. forced convection could be employed.

According to the Stefan-Boltzmann law an object does emit heat power in the form of electromagnetic waves dependent on its temperature, the ambient temperature and the surface emissivity. Heat transfer via radiation also works if there is no media surrounding the heat sink and therefore is the only relevant heat transfer mechanism e.g. for space applications.

2.2 Mathematical Model

In this section a mathematical model of heat conduction for calculating stationary and dynamic temperature distributions inside power semi-conductors and heat sinks will be derived. For simplification a one-dimensional structure (e.g. an isolated rectangular rod, cf. **Fig.1**, top-left) of homogenous material will be analyzed. The results gained could be expanded easily to three dimensions (see section 2.5).

According to the one-dimensional consideration the time-dependent temperature T is equally distributed over a cross-section A (called *Isotherm*) of the rod at a position x considered and the heat energy flow density q [W/m^2] is proportional to the negative local temperature gradient

$$q = -\lambda_{th} \frac{\partial T}{\partial x}. \tag{1}$$

The proportional factor called *thermal conductivity* λ_{th} [W/(K·m)] is a material property. Generally, heat flow density

and temperature gradient are vectors, but for the one-dimensional model the direction of the heat flow is aligned with the x-axis and therefore scalar values could be used.
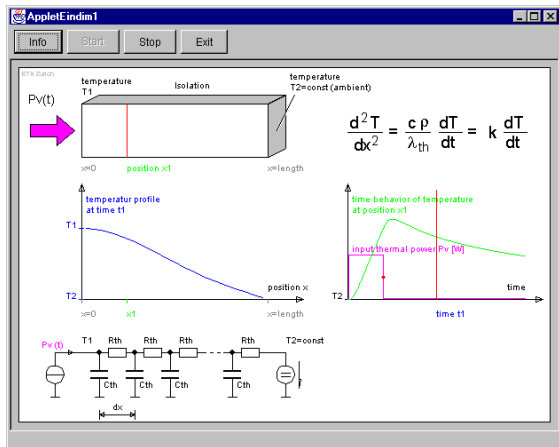

Fig.1: Interactive applet of *iPES-Thermal* for demonstrating the time-behavior and the position-dependency (profile) of the temperature for one-dimensional heat energy conduction as described by Eq.(4). The on-time of thermal input power pulse can be set with the mouse. Furthermore, a position x and an instant t_1 in time could be defined for investigating the temperature time behavior and profile.

For a finite volume element $\delta V = A \cdot \delta x$ located at coordinate x the thermal power $p(x)$ flowing into the volume element is partially heating up δV and partially transferred into the subsequent volume element

$$p(x) - p(x+\delta x) = q(x)\,A - q(x+\delta x)\,A =$$
$$= c\,\delta m\,\frac{\partial T}{\partial t} = c\,\rho\,A\,\delta x\,\frac{\partial T}{\partial t} \tag{2}$$

where δm [kg] denominates the mass of the volume element δV, ρ [kg/m³] specifies the material density, and c [Ws/(K·kg)] is the *specific thermal capacitance*. With a first-order Taylor-approximation of $p(x+\delta x)$ in (2) there results

$$-\frac{\partial q(x)}{\partial x} = c\,\rho\,\frac{\partial T}{\partial t}. \tag{3}$$

Considering (1) this finally results in the general *heat conduction (wave) equation* which provides the basis for all further calculations

$$\boxed{\frac{\partial^2 T}{\partial x^2} = \frac{c\,\rho}{\lambda_{th}}\frac{\partial T}{\partial t}}. \tag{4}$$

2.3 Electric Equivalent Circuit

For calculating stationary and dynamic temperature distributions inside power semiconductors and heat sinks, Eq.(4) has to be solved. This could be performed by mathematical concepts like the finite difference method (discussed in section 2.5). Alternatively, an electric equivalent circuit of the thermal system can be defined where concepts well known by electrical engineers could be employed for calculating the temperature time behavior and profile.

For transferring the thermal problem into an equivalent electric circuit problem we refer to an electric transmission line described by the partial differential equation

$$\frac{\partial^2 u}{\partial x^2} = C'_{el}\,L'_{el}\,\frac{\partial^2 u}{\partial t^2} + (C'_{el}\,R'_{el} + G'_{el}\,L'_{el})\frac{\partial u}{\partial t} + G'_{el}\,R'_{el}\,u\,. \tag{5}$$

For (ideal) transmission lines with no inductance ($L_{el}'=0$) and ideal isolation in between the two single lines ($G_{el}'=0$) we receive

$$\frac{\partial^2 u}{\partial x^2} = C'_{el}\,R'_{el}\,\frac{\partial u}{\partial t} \tag{6}$$

where C_{el}' [F/m] is the capacitance, and R_{el}' [Ω/m] the resistance per unit length. According to the mathematical analogy of Eqs.(4) and (6) the solution of (4) can be directly derived from (6).

Injecting heat power P_0 at $x=0$ and using (1), we have for *stationary* problems, i.e. for $\partial T/\partial t=0$, a *linear* temperature profile and/or

$$P_0 = q\,A = -\lambda_{th}\,A\,\frac{\partial T}{\partial x} = -\lambda_{th}\,A\,\frac{T_0 - T_l}{l}\,. \tag{7}$$

where $T_0 = T(x=0)$ and the given temperature at the end of the rod is $T_l = T(x=l)$. According to (6) the temperature T has to be interpreted as voltage u, and the injected heat power $P_0=q_0\cdot A$ could be interpreted as electric current i. With reference to Eq.(7) we correspondingly define a *thermal resistance* R_{th} [K/W] of the homogenous one-dimensional isolated rod of the length l

$$\boxed{R_{th,l} = \frac{l}{\lambda_{th}\,A}}, \tag{8}$$

where

$$P_0 = \frac{1}{R_{th}}(T_0 - T_l) \tag{9}$$

is valid. Based on the general relation for an electric capacitance

$$i(t)\,\partial t = C_{el}\,\partial u \tag{10}$$

we furthermore define a *thermal capacitance* C_{th} [Ws/K]

$$p(t)\,\partial t = C_{th}\,\partial T \tag{11}$$

of the homogenous rod, where considering Eqs.(4), (6),(8), and (11)

$$\boxed{C_{th} = c\,\rho\,A\,l} \tag{12}$$

and/or

$$\boxed{\frac{\partial^2 T}{\partial x^2} = R'_{th}\,C'_{th}\,\frac{\partial T}{\partial t}} \tag{13}$$

is valid. There, R'_{th} and C'_{th} denominate the thermal resistance and thermal capacitance per unit length of the rod. The analogy of the heat energy conduction problem to the electric transmission line problem now is immediately obvious (cf. Eqs.(4) and (13)).

2.4 Accuracy of the Equivalent Circuit Model

Using an electric equivalent circuit of the thermal system is especially convenient for analyzing multi-layer structures being characteristic for power semiconductors. There, for each (thin) layer i in a first approximation only one-dimensional heat conduction has to be considered. The equivalent circuit therefore directly reflects the layer structure where the material properties of each layer are considered by proper $R'_{th,i}$ and $C'_{th,i,}$ values (cf. Eqs.(8) and (12)). The solution of the electric problem then could be performed analytically or by a numerical circuit simulator (cf. section 2.6).

2.4.1 Stationary Behavior

For *stationary* problems the thermal capacitances $C_{th,i}$ can be omitted and each layer (each one-dimensional rod) can be described by a single thermal resistance $R_{th,i}$ corresponding to a linear temperature change inside the layer (see Eq.(7)).
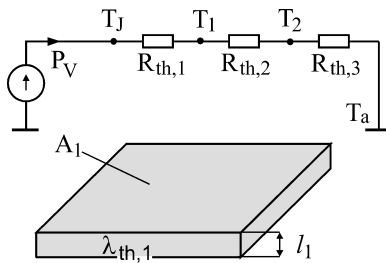

Fig.2: Equivalent electric circuit of three-layer one-dimensional heat energy conduction. One layer is shown below the electric equivalent circuit.

The temperatures (and/or voltages) T_J, T_1, T_2 at the equivalent circuit nodes represent the temperatures at the boundaries of different layers, the temperature T_a is the ambient temperature. The thermal power P_V (electric current) and/or the semiconductor power loss is injected into the top layer. Knowing the ambient temperature T_a one can easily calculate the power semiconductor junction temperature T_J, i.e. the temperature on top of the first layer.

In case the area where the power losses are applied is smaller than the cross section of the heat conducting material heat spreading does occur. There, the heat conducting cross section does increase in the direction of the heat propagation. For improving the accuracy of the calculation this can be taken into account by correction factors as discussed in [6].

2.4.2 Transient Behavior

For *dynamic* problems each layer has to be subdivided into several $R_{th}C_{th}$-cells in order to accurately represent the heat conduction mechanism being dependent on position and time (cf. Eq.(13)). Therefore, the resulting electric equivalent circuit of each layer comprises a series connection of these cell structures as shown in **Fig.3**(a) for five cells and in Fig.3(b) for only two cells.

It is obvious that with increasing number of cells the accuracy of the model will improve. On the other hand, the calculation effort (computation time) does increase, accordingly. Therefore, it is up to the engineer to make a decision between necessary, i.e. problem-specific accuracy and problem-solving effort.

The Java applet shown in Fig.3 allows to increase and decrease the number of cells employed for the modeling of a layer. A comparison against the exact solution provides an immediate impression of the modeling accuracy. Furthermore, the scaling of the time-behavior of the rod input temperature can be switched between logarithmic and linear (e.g. Fig.3 shows time-behavior in log-log scale) what does allow to evaluate the model accuracy over several decades in time.
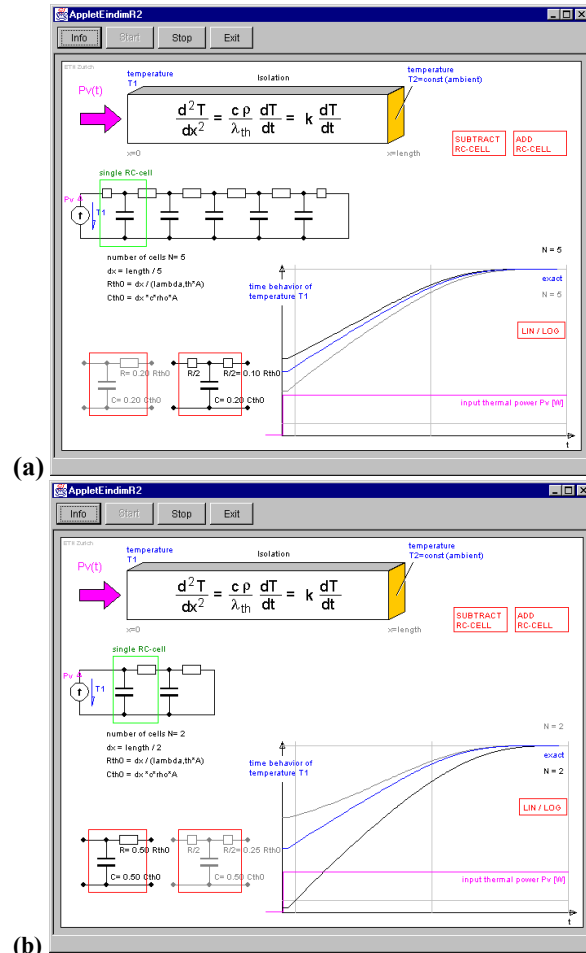

(a)

(b)

Fig.3: Interactive applet of *iPES-Thermal* for showing the dependency of the modeling accuracy of the electric equivalent circuit of the heat energy conduction in a layer of a multiple-layer power semiconductor in dependency on cell number and cell type. Cells can be added and subtracted with clicking the mouse, also the cell-type can be selected with the mouse.

Employing more than three cells already gives sufficiently accurate results. To further significantly increase the accuracy of the model each $R_{th}C_{th}$–cell (highlighted in Fig.3(b), bottom-left) could be changed into a T-type structure, $\frac{1}{2}R_{th}C_{th}\frac{1}{2}R_{th}$, highlighted in Fig.3(a), bottom-left. Alternatively, also a π-type cell structure, $\frac{1}{2}R_{th}$-C_{th}-$\frac{1}{2}R_{th}$, could be selected.

2.5 Finite Difference Method and $R_{th}C_{th}$-Equivalent Circuits for 2D and 3D Problems

For a three-dimensional problem we have to extend Eq.(4) to

$$\frac{\partial^2 T}{\partial x^2} + \frac{\partial^2 T}{\partial y^2} + \frac{\partial^2 T}{\partial z^2} = \frac{c\,\rho}{\lambda_{th}}\frac{\partial T}{\partial t}. \tag{14}$$

As the calculation time has to be minimized for animated simulation in order to give the user the impression of an immediate response to parameter changes, finite difference methods [5] are employed in *iPES-Thermal* for solving Eq.(14). As will be shown in the following this results in mathematically identical relations as for employing the electric equivalent circuit discussed in section 2.3. For the sake of clearness we will limit our considerations to the stationary temperature distribution, i.e. the thermal capacitances will be omitted.

2.5.1 Finite Difference Method

A temperature distribution in general is a continuous scalar function of position and time. For numerical calculation temperature values have to be defined at discrete positions and at discrete time instances.
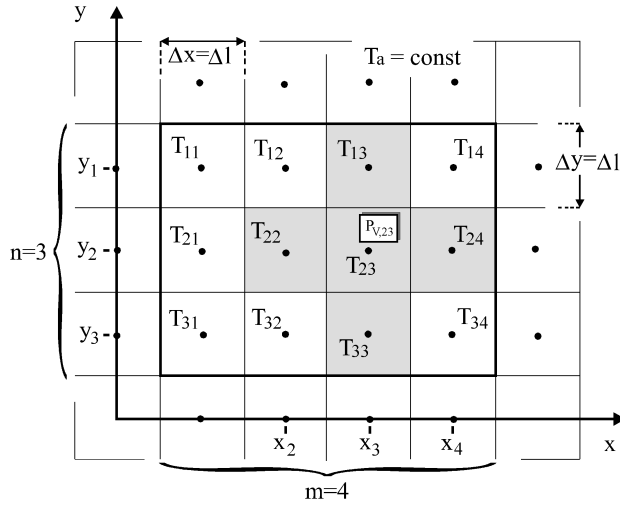

Fig.4: Partition of a geometry divided into $(n \times m)= 12$ rectangular-shaped cells for calculating the two-dimensional temperature-distribution based on the finite difference method. We assume a thermal power $P_{V,23}$ to be injected at cell *(23)*.

For the finite difference method the geometry is divided into rectangular cells and the unknown field quantities (temperatures) are referred to the center of these cells. This is shown in **Fig.4** for a two-dimensional temperature field, but can easily be extended into three dimensions. For calculating the temperature T_{23} we have to take the temperatures T_{22}, T_{33}, T_{24}, T_{13} of the neighboring elements into consideration. All five relevant elements are highlighted in Fig.4. The first and second deviation of the temperature can now be calculated using linear approximations

$$\left.\frac{\partial T}{\partial x}\right|_{y=y2,x=x3} = \frac{T_{23} - T_{22}}{\Delta x} \tag{15}$$

$$\left.\frac{\partial T}{\partial x}\right|_{y=y2,x=x4} = \frac{T_{24} - T_{23}}{\Delta x} \tag{16}$$

$$\left.\frac{\partial^2 T}{\partial x^2}\right|_{y=y2,x=x3} = \frac{1}{\Delta x}\left(\frac{T_{24}-T_{23}}{\Delta x} - \frac{T_{23}-T_{22}}{\Delta x}\right) = \frac{T_{22}+T_{24}-2\,T_{23}}{(\Delta x)^2} \tag{17}$$

$$\left.\frac{\partial T}{\partial y}\right|_{y=y2,x=x3} = \frac{T_{23} - T_{33}}{\Delta y} \tag{18}$$

$$\left.\frac{\partial T}{\partial y}\right|_{y=y1,x=x3} = \frac{T_{13} - T_{23}}{\Delta y} \tag{19}$$

$$\left.\frac{\partial^2 T}{\partial y^2}\right|_{y=y2,x=x3} = \frac{1}{\Delta y}\left(\frac{T_{13}-T_{23}}{\Delta y} - \frac{T_{23}-T_{33}}{\Delta y}\right) = \frac{T_{33}+T_{13}-2\,T_{23}}{(\Delta y)^2} \tag{20}$$

Substituting Eqs.(17) and (20) into (14), a discretization of the position is introduced but the temperature behavior is still continuous in time.

Considering a discretization in time as shown in **Fig.5** and considering e.g. the position $(y,x)=(y_2,x_3)$ and/or cell *(2,3)* we have temperature time-derivation to be introduced in the right hand side of Eq.(14)

$$\left.\frac{\partial T}{\partial t}\right|_{y=y2,x=x3} = \frac{T_{23}^{(k)} - T_{23}^{(k-1)}}{\Delta t} \tag{21}$$

where $T_{23}^{(k)}$ denotes the temperature value at time $t= k.\Delta t$ (Δt is the simulation time step) and $T_{23}^{(k-1)}=T_{23}(t=(k-1).\Delta t)$.

As can be clearly seen from Fig.5, the slope calculated in Eq.(21) should for best approximation be related to average value

$$T_{yx}^{(avg,(k-1)\rightarrow(k))} = \frac{T_{yx}^{(k)} + T_{yx}^{(k-1)}}{2}. \tag{22}$$

Therefore, we substitute for the temperature values in Eqs.(15)-(20) being still continuous in time

$$T_{yx} \rightarrow T_{yx}^{(avg,(k-1)\rightarrow(k))}. \tag{23}$$

There, one has to note, that the resulting set of equations will again only contain temperature values $T_{yx}^{(\xi)}$, $\xi=...(k-2),(k-1),k$ and/or cause low computational effort. However, due to Eq.(23) the discrete time-step Δt is effectively cut in half what does significantly increase the numerical stability and the accuracy of the algorithm.
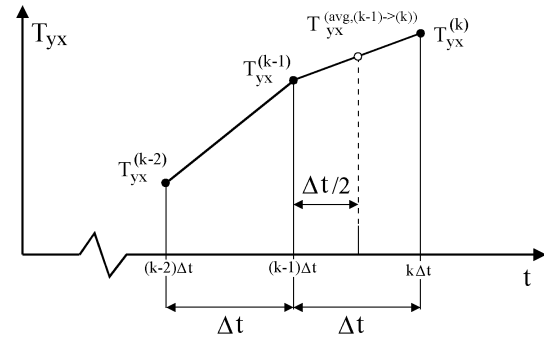

Fig.5: Time behaviour of temperature T_{yx} approximated for numerical simulation by temperature values at discrete time instances.

If the cells are defined to be of quadratic shape (Fig.4)

$$\Delta x = \Delta y = \Delta l \qquad (24)$$

there results a linear equation for the temperature of each cell of Fig.4

$$(\frac{c\,\rho}{\lambda_{th}}\frac{(\Delta l)^2}{\Delta t}+2)\,T_{23}^{(k)}-\frac{1}{2}(T_{22}^{(k)}+T_{33}^{(k)}+T_{24}^{(k)}+T_{13}^{(k)})= \qquad (25)$$

$$=(\frac{c\,\rho}{\lambda_{th}}\frac{(\Delta l)^2}{\Delta t}-2)\,T_{23}^{(k-1)}-\frac{1}{2}(T_{22}^{(k-1)}+T_{33}^{(k-1)}+T_{24}^{(k-1)}+T_{13}^{(k-1)})$$

Injecting thermal power P_V [W] into geometric cells is described by a boundary condition based on Eq.(7) as

$$\frac{\partial T}{\partial x}(0_+,t)=\frac{-p(x=0,t)}{\lambda_{th}\,A}=\frac{-p_0(t)}{\lambda_{th}\,A} \qquad (26)$$

$$\frac{\Delta T}{\Delta l}=\frac{-P_{V,23}}{\lambda_{th}\,A} \qquad (27)$$

$$\Delta T=-P_{V,23}\,\frac{\Delta l}{\lambda_{th}\,A}=-P_{V,23}\,R_{th} \qquad (28)$$

This boundary condition has to be considered in Eq.(25) by adding the term defined in Eq.(28) as

$$(\frac{c\,\rho}{\lambda_{th}}\frac{(\Delta l)^2}{\Delta t}+2)\,T_{23}^{(k)}-\frac{1}{2}(T_{22}^{(k)}+T_{33}^{(k)}+T_{24}^{(k)}+T_{13}^{(k)})-P_{V,23}R_{th}^{(23)} \qquad (29)$$

$$=(\frac{c\,\rho}{\lambda_{th}}\frac{(\Delta l)^2}{\Delta t}-2)\,T_{23}^{(k-1)}-\frac{1}{2}(T_{22}^{(k-1)}+T_{33}^{(k-1)}+T_{24}^{(k-1)}+T_{13}^{(k-1)})$$

In the following it will be shown how to set up the linear equation system for the numerical calculation of the temperature distribution over the whole geometry.

As only the *stationary* conditions are considered in the following Eq.(29) is reduced to

$$\frac{\partial T_{yx}}{\partial t}=0\rightarrow 4\,T_{23}-(T_{22}+T_{33}+T_{24}+T_{13})=P_{V,23}R_{th} \qquad (30)$$

$$\underbrace{\begin{pmatrix} 4 & -1 & .. & 0 & 0 \\ -1 & 4 & .. & 0 & 0 \\ .. & .. & .. & .. & .. \\ 0 & 0 & .. & 4 & -1 \\ 0 & 0 & .. & -1 & 4 \end{pmatrix}}_{12\times12 \;\; MATRIX\;\underline{A}}\underbrace{\begin{pmatrix} T_{11} \\ T_{12} \\ .. \\ T_{33} \\ T_{34} \end{pmatrix}}_{\underline{T}}=\begin{pmatrix} 2T_a \\ T_a \\ .. \\ T_a \\ 2T_a \end{pmatrix} \qquad (31)$$

As Fig.4 shows, a geometry subdivided into *(mxn)*= (3x4) cells results in *(n.m)*=(3·4)=12 unknown temperature values. Defining equations systematically for each cell as described in Eq.(30) we finally get a matrix equation

The 7th row of the (12x12)-matrix $\underline{A}$ of Eq.(31), corresponding with temperature T_{23}, is defined as

$$\underline{A}^{(j=7)} = (0;\ 0;\ -1;\ 0;\ 0;\ -1;\ 4;\ -1;\ 0;\ 0;\ -1;\ 0) \qquad (32)$$

(the matrix index *(ji)* defines the position of the element within the (12x12)-matrix; *j=1…12* indicating the row, *i=1…12* is the column index) if the vector of unknown temperatures is defined as

$$\underline{T}^T =(T_{11};T_{12};T_{13};T_{14};T_{21};T_{22};T_{23};T_{24};T_{31};T_{32};T_{33};\ T_{34}) \ . \qquad (33)$$

The diagonal of the coefficient matrix in Eq.(31) is comprised by "+4" entries. Each geometric cell has got four direct neighbors contributing four "-1" entries in each row of the matrix. This is shown for cell *(23)* with its neighboring cells *(13),(22),(24),(33)* in Eqs.(32) and (33). All other elements of the row are zero resulting in a sparse matrix. On the other hand, for example, cell *(13)* is located at the boundary of the geometric structure in Fig.4 and therefore does have only three immediate neighbours *(12),(14),(23)* contributing "-1" entries in the 3rd row of the matrix. The temperature of the cell neighbouring in the positive *x*-direction is equal to the known ambient temperature T_a; therefore this cell has not been given a coordinate and does contribute an entry T_a in the right-hand side (disturbance) vector of Eq.(31).

According to Eq.(30) thermal power injected into a certain cell results in an entry $P_{V,yx}\cdot R_{th}$ into the right-hand disturbance vector of Eq.(31) in the row of this cell.
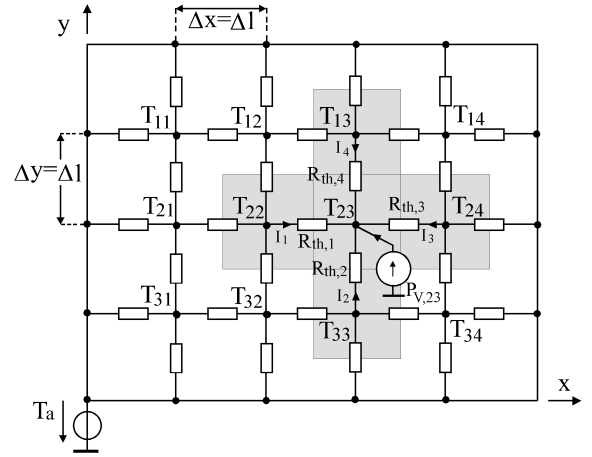

Fig.6: Electric equivalent circuit for the calculation of a two-dimensional stationary temperature distribution for given ambient temperature T_a=const and given power losses, i.e. injecting current $P_{V,23}$ at cell *(23)*.

2.5.2 $R_{th}C_{th}$ Equivalent Circuits

For calculating a two- (or three-)dimensional *stationary* temperature distribution it is also possible to refer to an electric equivalent circuit as introduced in section 2.3 for one-dimensional heat energy conduction. As in section 2.5.1 we also will consider only the stationary temperature distribution in the following and/or omit the thermal capacitances. The geometry is again divided into cells (cf. **Fig.6**) which directly correspond to the partitioning shown in Fig.4. The power $P_{V,23}$ is injected into the cell numbered *(23)* by a current source.

For the network in Fig.6 we can directly have

$$I_1 + I_2 + I_3 + I_4 + I_{PV,23} = 0\,, \qquad (34)$$

$$I_1 = \frac{T_{22} - T_{23}}{R_{th,1}}\,, \qquad (35)$$

$$R_{th,1} = R_{th,2} = R_{th,3} = R_{th,4} = \frac{\Delta l}{\lambda_{th}\,A}\,, \qquad (36)$$

$$4\,T_{23} = (T_{22} + T_{33} + T_{24} + T_{13}) + R_{th}\,P_{V,23} =$$
$$= (T_{22} + T_{33} + T_{24} + T_{13}) + \frac{\Delta l}{\lambda_{th}\,A}\,P_{V,23} \qquad (37)$$

Comparing Eq.(37) to Eq.(30) it is obvious that both methods, i.e. the finite difference method and the electric equivalent circuit do result in an identical set of equations and are therefore mathematically equivalent.

2.6 Coupling of Electric Power Circuit Simulation and Thermal Simulation

Software packages available for the simulation of electric circuits do set up internally an equation system for a circuit considered and do provide the time-behavior of voltages of all nodes and currents through all components.

As the temperature often takes significant influence on the properties of a power electronic circuit it is desirable, e.g. to calculate the power semiconductor junction temperatures and to continuously update the power semiconductor models employed in the circuit simulation.
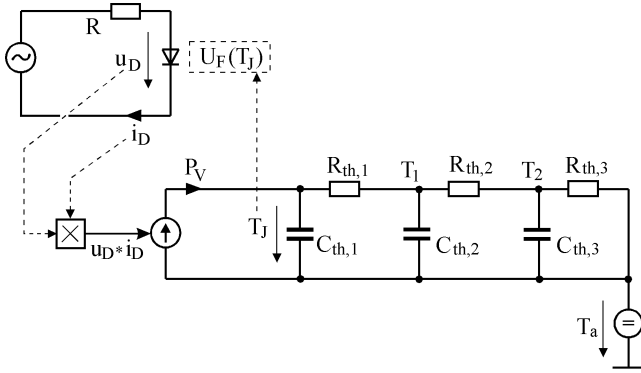

Fig.7: Simultaneous coupling of the simulation of the power circuit and of the thermal electric equivalent circuit shown for a single diode rectifier.

This can be achieved by using the electric equivalent circuits of the thermal properties of the components which could be directly integrated into the circuit simulation. The basic principle is shown in **Fig.7** for a single diode rectifier circuit. There, the diode power losses P_V are impressed by a controlled current source, where P_V is the product of the diode voltage u_D and current i_D. The thermal electric equivalent circuit is defined according to the transient thermal impedance provided in the diode data sheet (cf. section 3). The ambient temperature T_a is defined by a DC-voltage source. The semiconductor junction temperature T_J does take influence on the conduction voltage drop $U_F = U_F(T_J)$ and/or on the semiconductor power losses.

For the simulator the thermal equivalent circuit is just another electric circuit to be analyzed. Therefore, no software of special type is required for calculating the temperature stress T_J (interpreted as a voltage in the model). More information on this simple and effective concept can be found e.g. in [4] and [6].

3 Transient Thermal Impedance

The stresses on the power semiconductors employed in power converters are in general varying over time according to changing load conditions, alternating input or output voltage/current and operating parameter dependent switching frequency. Therefore, the instantaneous power losses could show a significant deviation form the average value.

Accordingly, the calculation of the maximum power semiconductor junction temperature which is to a large extent determining the failure-rate and/or reliability has to be performed based on a dynamic thermal model of the system like described in section 2.2. There, instead of solving Eq.(4) the analysis could be based on the *transient thermal impedance* $Z_{th}(t)$ which is given in the power semiconductor data sheet and does show the time behavior of the junction temperature $T_J = T_O$ in reaction to a step-like change of the semiconductor power losses.

3.1 Definition of Transient Thermal Impedance

In order to show the physical background of the definition of $Z_{th}(t)$, we will analytically calculate the transient thermal impedance for one-dimensional heat conduction in an isolated rod of infinite length in the following.

For solving the differential equation (13) analytically, we apply the Laplace transformation

$$\frac{d^2 T}{dx^2} - R'_{th}\,C'_{th}\,s\,T = 0 \qquad (38)$$

and with

$$T = C\,e^{\alpha x} \qquad (39)$$

we then receive the characteristic equation

$$\alpha^2 - s\,R'_{th}\,C'_{th} = 0 \qquad (40)$$

with solutions

$$\alpha_{12} = \pm\sqrt{R'_{th}\,C'_{th}}\ \sqrt{s} \qquad (41)$$

(where the Laplace variable s is only a parameter) resulting in a temperature profile

$$T(x,s) = C_1\,e^{+x\sqrt{R'_{th}\,C'_{th}}\,\sqrt{s}} + C_2\,e^{-x\sqrt{R'_{th}\,C'_{th}}\,\sqrt{s}} =$$
$$= \frac{R'_{th}}{\sqrt{R'_{th}\,C'_{th}}}\,\frac{1}{\sqrt{s}}\,e^{-x\sqrt{R'_{th}\,C'_{th}}\,\sqrt{s}}\,P_0(s) \qquad (42)$$

where a power $p_0(t)$ being injected at $x=0$

$$\frac{\partial T}{\partial x}(0_+, t) = -p(x=0,t)\,R_{th}' = -p_0(t)\,R_{th}' \qquad (43)$$

is assumed. In Eq.(42) the surface (junction) temperature is of most interest

$$T(x=0, s) = T_0(s) = \frac{R'_{th}}{\sqrt{R'_{th}\,C'_{th}}}\,\frac{1}{\sqrt{s}}\,P_0(s) \cdot \qquad (44)$$

Considering the electric equivalent circuit of the thermal system we now could define a circuit input impedance

$$Z_{th}(s) = \frac{T_0(s)}{P_0(s)} = \frac{R'_{th}}{\sqrt{R'_{th}\,C'_{th}}}\,\frac{1}{\sqrt{s}} = \sqrt{\frac{R'_{th}}{C'_{th}}}\,\frac{1}{\sqrt{s}} \qquad (45)$$

which, however must not be confused with the transient thermal impedance $Z_{th}(t)$.

For the calculation of $Z_{th}(t)$ we assume for $p_0(t)$ a step-like time behavior, $p_0(t)=P_0$, and therefore have in the Laplace domain

$$P_o(s) = \frac{P_0}{s} \cdot \qquad (46)$$

With reference to Eq.(45) the resulting transient behavior of the temperature is

$$T_0(s) = P_0(s)\, Z_{th}(s) = P_0 \sqrt{\frac{R'_{th}}{C'_{th}}} \frac{1}{s\sqrt{s}} \qquad (47)$$

and in the time domain

$$T_0(t) = P_0\, R'_{th} \sqrt{\frac{4}{\pi} \frac{t}{R'_{th}\,C'_{th}}} \cdot \qquad (48)$$

For characterizing the transient thermal behavior we now define the *transient thermal impedance* as

$$Z_{th}(t) = \frac{T_0(t)}{P_0}, \qquad (49)$$

which physically represents the step-response of the junction temperature T_0 normalized to the thermal input power P_0. In the case of one-dimensional heat conduction this results in

$$Z_{th}(t) = R'_{th} \sqrt{\frac{4}{\pi} \frac{t}{R'_{th}\,C'_{th}}} = R_{th} \sqrt{\frac{4}{\pi} \frac{t}{R_{th}\,C_{th}}} \qquad (50)$$

where R'_{th} and C'_{th} could be replaced by the absolute values R_{th} and C_{th} of a section of the rod.

3.2 Simple Transient Thermal Models

Based on Eq.(49) e.g. the time-behavior of the temperature drop T_l occurring across a heat conducting layer of stationary thermal resistance $R_{th,l}$, e.g. the isolating layer of a power semiconductor can be approximated without solving Eq.(13) analytically or numerically,

Showing Eq.(48) in log-log scaling

$$\log\!\left(\frac{T_0}{P_0\,R_{th,l}}\right) = \frac{1}{2}\log\!\left(\frac{4}{\pi}\right) + \frac{1}{2}\log\!\left(\frac{t}{R_{th,l}\,C_{th,l}}\right) \qquad (51)$$

it is immediately obvious that the slope of the temperature change over time for a layer of infinite thickness is *10dB/dec*. We now could directly define an approximation of the normalized time-behavior of T_0 and/or of the transient thermal impedance considering that T_0 in the stationary case will assume a value $T_l = P_0\,R_{th,l}$, if the rod is not of infinite but of finite length l

$$Z_{th,l}(t) = \begin{cases} R_{th,l}\,\sqrt{t/\tau_{th,l}} & \text{for} \quad t \ll \tau_{th} \\ R_{th,l} & \text{for} \quad t \gg \tau_{th} \end{cases} \qquad (52)$$

(cf. **Fig.8**) where

$$\tau_{th,l} = \frac{\pi}{4} R_{th,l}\,C_{th,l} = \frac{c\rho}{\lambda_{th}} l^2 \qquad (53)$$

has to be considered as the thermal time-constant of the layer. For $t < \tau_{th}$ the temperature T_0 does exhibit a behavior being characteristic for a layer of infinite thickness, for $t > \tau_{th}$ the layer could be considered as having reached a stationary thermal condition which is characterized by a constant gradient of the temperature and/or by the thermal resistance $R_{th,l}$.
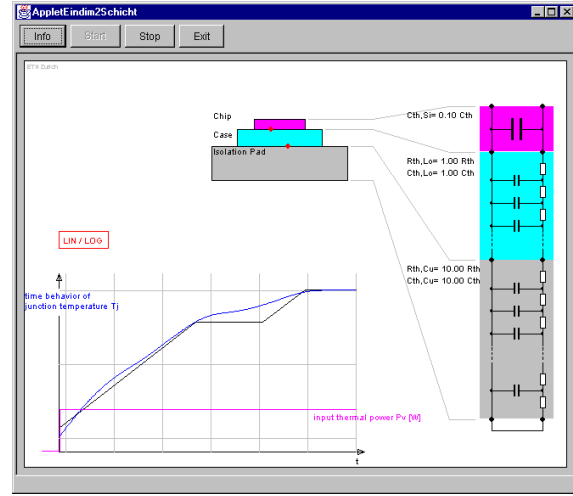

Fig. 8: Interactive applet of *iPES-Thermal* for showing the exact transient thermal impedance of a multiple-layer thermal structure in comparison to the asymptotic solution according to Eqs.(52) and (54). The thickness of the layers can be changed with the mouse.

As in power semiconductors the power losses do occur in a finite volume inside the silicon die showing a thermal capacitance $C_{th,j}$ we have to consider in addition to Eq.(52) a thermal impedance

$$Z_{th,j}(t) = \frac{T_j(t)}{P_0} = \frac{t}{C_{th,j}} \cdot \qquad (54)$$

In log-log scaling the slope of the temperature change over time resulting for a power pulse P_0 then is *20dB/dec*.

For a detailed discussion of combining Eq.(52) and Eq.(54) to the asymptotic approximation of the transient thermal impedance of a multiple-layer thermal structure (cf. Fig.8) we would like to refer to [7] for the sake of brevity.
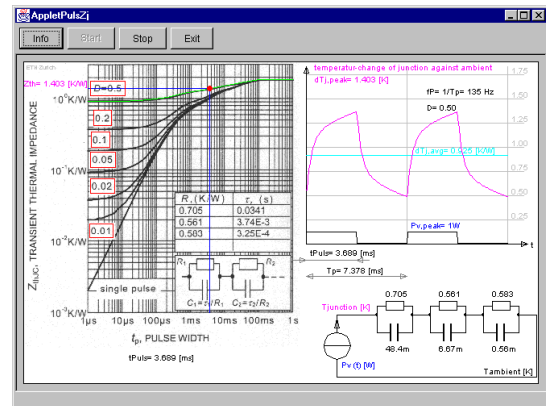

Fig.9: Interactive applet of *iPES-Thermal* for showing the transient thermal impedance of a power semiconductor and the related time-behavior of the junction temperature for applying a periodic power loss pulse of duty-cycle $D=[0\ldots1]$. There, the transient thermal impedance is defined based on the peak value of the normalized junction temperature occurring within the power pulse duration t_P. The operating point (D, t_P) can be changed with the mouse.

3.3 $Z_{th}(t)$ Specification in Data Sheets

In **Fig.9**, left-hand side, a Java applet of *iPES-Thermal* shows the transient thermal impedance of a power semiconductor in log-log scale as typically depicted in a data sheet. The width t_P of a rectangular periodic thermal input power pulse with a normalized amplitude of 1.0W is given on the horizontal axis; the time-behavior corresponding to a selected pulse duty cycle D and pulse-width t_P is shown on right-hand side. The equivalent thermal circuit model is shown bottom-right.

3.4 Cauer-Type and Foster-Type Electric Equivalent Circuits

In case $Z_{th}(t)$ of a power semiconductor is known from a data sheet or measurement, the Parameters $R_{th,i}$, $C_{th,i}$ of the thermal system can be identified in analogy to the identification of a dynamic system in control engineering based on a step-response [4]. The different time constants then could easily be combined in a Foster-type electric equivalent circuit as shown in **Fig.10**(b). The simplicity of this procedure makes the Foster-type circuit an attractive choice for power semiconductor manufacturers (cf. Fig.9). However, the Foster-type circuit only does correctly describe the junction temperature time behavior and does *not* provide information on the inner temperature distribution. If, for example, a pulse of thermal power is injected at the input the temperature at all internal nodes will change immediately due to the capacitors C_{th1}, C_{th2}, C_{th3} forming a series-connection between the input- and the output-side. This is clearly different from reality, where the propagation of the temperature increase from the layer surface is with a time-delay (cf. Eq.(52)). Also, the thermal energy stored inside a layer volume is proportional to the absolute temperature as modelled by the Cauer-type circuit (cf. Fig.9(a)), but is shown to be proportional to the temperature differences of the nodes for the Foster-type circuit.

Therefore, the Foster-type circuit is restricted to the specific application given in the data sheet and cannot be extended easily, i.e. *all* parameters would have to be changed each time the thermal system is extended. In contrast the Cauer-type circuit does describes the physical properties correctly and does allow to add models of further layers by series connection.
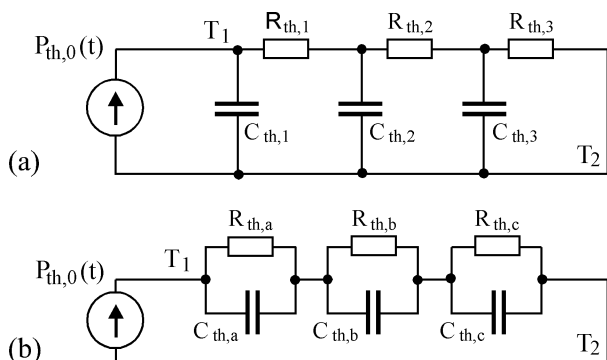

Fig.10: (a) Cauer-type and **(b)** Foster-type electric equivalent circuit a one-dimensional heat conducting layer.

4 Conclusions

The educational module *iPES-Thermal*, being part of the *Interactive Power Electronics Seminar* (available at no costs at www.ipes.ethz.ch), does comprise Java applets on basics of thermal issues of power electronic system. This paper presents in tutorial style an abridged version of the accompanying lecture notes. A comprehensive version of the text will be published in near future in a textbook on *Lectures on Fundamentals of Power Electronics*.

5 References

[1] **Drofenik, U., and Kolar, J. W.:** *Interactive Power Electronics Seminar (iPES)* at www.ipes.ethz.ch .

[2] **Drofenik, U., and Kolar, J. W.:** *Interactive Power Electronics Seminar (iPES) – A Web-Based Introductory Power Electronics Course Employing Java-Applets.* Proc. of the 33rd IEEE Power Electronics Specialists Conference, Cairns, Australia, June 23-27, Vol. 2, pp. 443-448 (2002).

[3] **Mohan, N., Undeland, T.M., and Robbins, W.P.:** *Power Electronics.* John Wiley & Sons, 2002. ISBN: 0471226939 (2002).

[4] **Jakopovic, Z., Sunde, V., and Bencic, Z.:** *From Transient Thermal Impedance Measurement to Successful Electrothermal Simulation.* Proceedings of the 10th International Power Electronics and Motion Control Conference, Dubrovnik, Croatia, Sept. 9 - 11, CD-ROM, ISBN: 953-184-047-4 (2002).

[5] **Sykulski, J. K.:** *Computational Magnetics.* First Edition. Chapman & Hall, 1995, ISBN 0 412 58570 7.

[6] **März, M., and Nance, P.:** *Thermal Modelling of Power-Electronic Systems.* Published at www.iis-b.fhg.de/en/arb_geb/powersys_pub.htm

[7] **Newell, W.E.:** *Transient Thermal Analysis of Solid-State Power Devices – Making a Dreaded Process Easy.* IEEE Transactions on Industry Applications, Vol. IA-12, No. 4, pp. 405-420 (1976).